BIOCHEMISTRY
including biophysical chemistry & molecular biology

Article

pubs.acs.org/biochemistry

Allosterically Regulated Unfolding of the A′α Helix Exposes the Dimerization Site of the Blue-Light-Sensing Aureochrome-LOV Domain

Elena Herman and Tilman Kottke*

Department of Chemistry, Physical and Biophysical Chemistry, Bielefeld University, Universitätsstraße 25, 33615 Bielefeld, Germany

Supporting Information

ABSTRACT: Aureochromes have been shown to act as blue-light-regulated transcription factors in algae in the absence of phototropins. Aureochromes comprise a light-, oxygen-, or voltage-sensitive (LOV) domain as a sensory module binding the flavin chromophore and a basic region leucine zipper (bZIP) domain as an effector. The domain arrangement in aureochromes with an N-terminal effector is inversed to other LOV proteins. To clarify the role of the linking A′α helix in signaling, we have investigated the LOV domain of aureochrome1a from the diatom alga *Phaeodactylum tricornutum* without the N-terminal A′α helix but with the C-terminal Jα helix. Results were analyzed in comparison to those previously obtained on the LOV domain with both flanking helices and on the LOV domain with the A′α helix but without the Jα helix. Fourier transform infrared difference spectroscopy provides evidence by a band at 1656 cm^{-1} that the A′α helix unfolds in response to light. This unfolding takes place only in the presence and as a consequence of the unfolding of the Jα helix, which points to an allosteric regulation. Size exclusion chromatography shows the LOV domain to be dimeric in the absence and monomeric in the presence of the A′α helix, implying that the folded helix covers the dimerization site. Therefore, the A′α helix directly modulates the oligomerization state of the LOV domain, whereas the Jα helix acts as an allosteric regulator. Both the allosteric control and the light-induced dimerization have not been observed in phototropin-LOV2 and point to a different signaling mechanism within the full-length proteins.

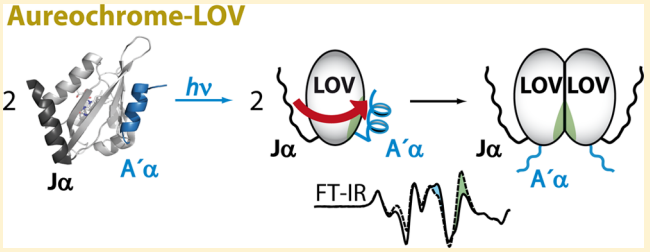

Aureochromes were discovered as a new type of blue-light receptor in the stramenopile alga *Vaucheria frigida*, in which they mediate blue-light-induced branching and the development of the sex organ.[1] Since then, a growing number of aureochromes from other photosynthetic stramenopile algae have been investigated.[2−4] In the diatom *Phaeodactylum tricornutum,* aureochrome1a was shown to repress high-light acclimation[3] and to induce cell division light-dependently.[5] Aureochrome from the brown alga *Saccharina japonica* was associated with blue-light-mediated photomorphogenesis during the growth and early development of sporophytes.[4] Interestingly, aureochromes have been found only in organisms that do not express phototropin, which acts as a blue-light receptor in higher plants, ferns, mosses, and green algae.[6]

Aureochromes are the first example of a blue-light-sensory LOV (light-, oxygen-, or voltage-sensitive) domain coupled to an N-terminal bZIP (basic-region leucine zipper) domain[7] (Figure 1A). LOV domains noncovalently bind flavin mononucleotide (FMN). Blue-light absorption leads to the reversible formation of a covalent adduct of FMN with a nearby cysteine residue as the signaling state (Figure 1B).[8] bZIP domains are DNA-binding domains exclusively found in eukaryotes and constitute one of the largest transcription factor families.[9,10] Accordingly, aureochromes function as blue-light-regulated transcription factors.[1] In support of this claim, monomeric aureochrome was demonstrated to dimerize upon illumination, which increased its affinity for DNA binding.[11] Furthermore, the vibrational signature of aureochrome is altered characteristically by illumination in the presence of DNA, which was attributed to the change in interaction with lysine and arginine side chains.[12]

Aureochrome exhibits an atypical domain topology (Figure 1A). To the best of our knowledge, aureochrome is the only LOV protein besides the putative helix−turn−helix (HTH)-LOV protein from *Sulfurimonas denitrificans* (Tmden_2087/uniprot Q30NS0)[7] that comprises an N-terminal but no C-terminal effector domain.[7,13,14] Therefore, aureochrome represents a unique eukaryotic LOV protein with an inverse domain order of sensor and effector. Moreover, the crystal structure of *V. frigida* aureochrome1-LOV points to a different positioning of the flanking helices as compared to that in phototropin-LOV2.[15] Accordingly, the authors postulated that aureochrome-LOV domains might offer new possibilities for optogenetics. Indeed, the LOV domains of aureochromes were successfully fused C-terminally to receptor tyrosine kinases mimicking the naturally occurring domain order. The fusion led

Received: December 11, 2014
Revised: January 26, 2015
Published: January 26, 2015

DOI: 10.1021/bi501509z
Biochemistry 2015, 54, 1484−1492

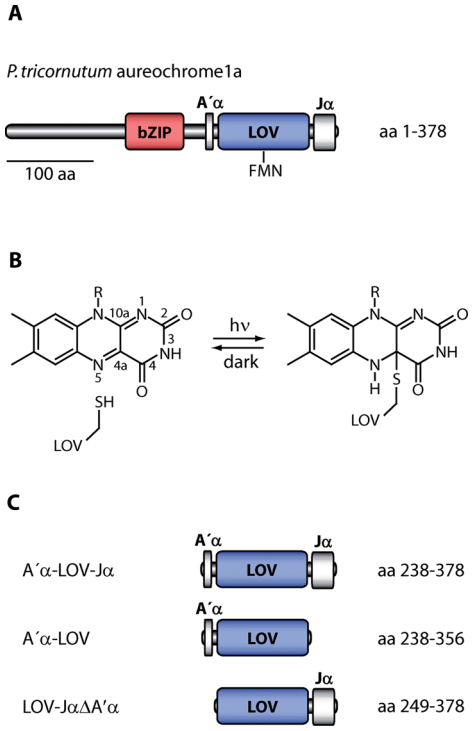

Figure 1. (A) Domain topology of aureochrome1a from *P. tricornutum*, which contains an N-terminal bZIP effector domain and a C-terminal LOV core domain with flanking helices A′α and Jα. (B) Chemical structures of the flavin chromophore in the LOV domain. In the dark, the flavin is in its oxidized state. Illumination with blue light leads to a reversible formation of a covalent adduct between the flavin and a nearby cysteine. (C) Schematic illustration of LOV domains of aureochrome1a investigated in this study (LOV-J$\alpha\Delta$A′α) and in a previous study (A′α-LOV-Jα and A′α-LOV).[17] LOV-J$\alpha\Delta$A′α contains the LOV core domain and the C-terminal flanking Jα helix but lacks the N-terminal flanking A′α helix.

to a light-dependent homodimerization and activation of cellular signaling in human cancer and endothelial cells in a magnitude comparable to that by a ligand.[16]

More importantly, the domain inversion raises the question of the role of the flanking A′α and Jα helices of the LOV domain in transmission of the signal to the bZIP domain (Figure 1A). It has been shown previously for the Jα helix of the isolated LOV domain that despite its C-terminal location an unfolding upon illumination is observed,[17] which is similar to the process activating the kinase of plant phototropins.[18,19] This unfolding is prerequisite for the light-induced dimerization of aureochrome-LOV.[17] The well-conserved N-terminal A′α helix began only recently to attract attention with regard to its role in signaling in phototropin. Mutations in the A′α helix of phototropin-LOV2 from *Chlamydomonas reinhardtii* resulted in a substantially reduced repressive activity of LOV2 on the kinase domain in the dark.[20] In tomato, a single mutation within the A′α helix led to impairment of most of the phototropin-mediated responses.[21] Zayner et al. observed by CD and fluorescence spectroscopy that the absence of the A′α helix in phototropin1-LOV2 from *Avena sativa* resulted in a partial undocking of the Jα helix in the dark.[22] Furthermore, light-induced unfolding of both the Jα helix and the A′α helix takes place regardless of the absence of the other helix. These observations suggested that the undocking of the A′α helix modulates that of the Jα helix.[22] In contrast, transient grating experiments demonstrated that unfolding of the Jα helix (τ = 1 ms) takes place much faster than A′α unfolding (τ = 12 ms).[23] The latter experiments were conducted on mutants of phototropin1-LOV2 from *Arabidopsis thaliana* that rendered one of the helices unfolded already in the dark and point to an independent activation of both helices in phototropin.

The A′α helix in aureochrome might play a decisive role in signaling, because it connects the sensory LOV domain via the linker region to the bZIP effector domain. In this study, we investigated the LOV domain of aureochrome1a, one of the four aureochromes found in the diatom *P. tricornutum*.[24] Diatoms contribute significantly to global photosynthetic carbon fixation.[25] The LOV domain was obtained with the Jα helix but lacking the A′α helix and was studied by UV−vis spectroscopy, FT-IR difference spectroscopy, and size exclusion chromatography. The results were analyzed by comparison to those previously obtained on the LOV domain with the A′α helix but lacking the Jα helix and on the LOV domain with both flanking helices.[17] Hereby, we identified the marker band for A′α unfolding in the infrared spectrum and observed that the A′α helix plays a key role in the photoresponse of the aureochrome-LOV domain by modulating its oligomeric state.

MATERIALS AND METHODS

Expression Construct. The vector encoding LOV-J$\alpha\Delta$A′α (amino acids 249−378) was generated by using pET28a (+)-A′α-LOV-Jα (amino acids 238−378) of aureochrome1a from *P. tricornutum*[17] as a polymerase chain reaction template. Nucleotides encoding the A′α helix (amino acids 238−248) were excluded by amplification using the 5′-end-phosphorylated forward and reverse primers 5′-p-CAG CAA AAC TTC GTC GTG ACC GAT CCG TCA TTG-3′ and 5′-p-CAT ATG GCT ACC GCG CGG CAC-3′ (Invitrogen) and Phusion polymerase (New England Biolabs). After *Dpn*I digestion, the vector fragment was ligated using T4 DNA ligase. The resulting sequence of the vector was verified by sequencing (GATC, Biotech).

Expression and Purification. Heterologous expression in *Escherichia coli* BL21(DE3) pLysE and purification via His-bind resin (Novagen) were performed as described previously.[17] After purification, LOV-J$\alpha\Delta$A′α was reconstituted with flavin mononucleotide (FMN) by incubation at twice the concentration of FMN with respect to protein for 2 h at 4 °C in the dark. To remove free FMN and imidazole, the protein was dialyzed three times against 400 volumes of 50 mM phosphate buffer (pH 8), 300 mM NaCl, and 20% glycerol. The purity of the protein was >95%, as judged by sodium dodecyl sulfate−polyacrylamide gel electrophoresis (SDS−PAGE) (Figure S1 of the Supporting Information). Reconstitution with FMN led to an increase in chromophore occupancy from 20 to 30% as determined by UV−vis spectroscopy.

UV−Vis Spectroscopy. UV−vis spectra were recorded on a Shimadzu UV-2450 spectrometer. Absorbance spectra were recorded before and after illumination for 10 s. Samples were illuminated with an LED with emission at 455 nm [20 nm full width at half-maximum (fwhm)] and an intensity of 20 mW cm^{-2} at the sample (Philips Lumileds). Kinetic traces were recorded in the dark at 447 nm and 20 °C after illumination for 500 ms. Absorbance spectra recorded in the dark were used for determination of the chromophore and protein concentration. Extinction coefficients of 12500 L mol^{-1} cm^{-1} at 450 nm[26] and 18500 L mol^{-1} cm^{-1} at 280 nm were used for free FMN, and an extinction coefficient of 10810 L mol^{-1} cm^{-1} was used for

DOI: 10.1021/bi501509z
Biochemistry 2015, 54, 1484−1492

the apoprotein at 280 nm as calculated with EXTCOEF (http://www.workbench.sdsc.edu).

Size Exclusion Chromatography. Aliquots of 60 μL with total protein concentrations of 0.2, 0.5, and 2.5 mM were analyzed via size exclusion chromatography with detection at 448 and 390 nm. Chromatography was performed at 4 °C using an Äkta purifier (GE Healthcare) and a Superdex75 10/300 GL column (GE Healthcare). The column was either in the dark or continuously illuminated using four LEDs (455 nm, 20 nm fwhm, Philips Lumileds). For equilibration and elution, 50 mM phosphate buffer (pH 8) and 300 mM NaCl were used. Protein samples were centrifuged at 21400*g* for 10 min at 4 °C before being loaded onto the column. Elution was performed with a flow rate of 0.4 mL/min. The apparent molecular mass of the sample was determined by calibration using standard marker proteins (GE Healthcare).

FT-IR Spectroscopy. The protein sample was transferred into 50 mM phosphate buffer (pH 8) and 100 mM NaCl via repeated ultrafiltration using a Vivaspin 500 filter device with a cutoff of 5 kDa (Sartorius). Finally, the sample was concentrated to ∼2.4 mM with respect to the bound chromophore (OD_{448} ∼ 30), which corresponds to a total protein concentration of ∼8.9 mM. Two microliters of the protein solution was applied onto a BaF_2 window and that window sealed with a second window without any drying. FT-IR difference spectra were recorded on Bruker IFS 66v and IFS 66/S spectrometers with long wave pass filters with cut-ons at 4.9 μm (OCLI) and 5.3 μm (Spectrogon), respectively, in front of the detector to block stray light and improve the signal-to-noise ratio. FT-IR difference spectra with a resolution of 2 cm^{-1} were recorded at 20 °C with 1024 scans before and after illumination for 2 s with a 455 nm LED (20 nm fwhm) with 20 mW cm^{-2} at the sample (Philips Lumileds). Several experiments with independent preparations were averaged to a total number of 10240 scans. FT-IR difference spectra were scaled to isolated chromophore bands at 1303, 1272, and 1251 cm^{-1}. Reconstitution with FMN did not alter the FT-IR difference spectrum (Figure S2 of the Supporting Information). Hydrogen/deuterium (H/D) exchange of A′α-LOV-Jα was performed by transferring the sample via ultrafiltration into 50 mM phosphate buffer in D_2O [pD 8.0 (pH 7.6)] and 100 mM NaCl. After concentration, the samples were kept in the BaF_2 cuvettes for at least 24 h at room temperature. FT-IR difference spectra were recorded as described above. Several experiments with independent preparations were averaged to a total number of 13312 scans.

RESULTS

The core LOV domain with a C-terminal Jα helical element but lacking the N-terminal A′α helix (termed LOV-JαΔA′α) of aureochrome1a from *P. tricornutum* (*Pt*AUREO1a) was heterologously expressed in *E. coli* and obtained as soluble and yellow protein. The UV−vis spectrum of the dark form shows the typical fine structure of a protein-bound chromophore in its oxidized state with absorption maxima at 448, 375, and 358 nm (Figure 2). After blue-light illumination for 10 s, the oxidized flavin was completely converted into the adduct state indicated by an absorption maximum at 390 nm (Figure 2). The recovery kinetics of LOV-JαΔA′α was recorded at 447 nm in the dark after blue-light illumination for 500 ms. Kinetic traces were fit using a biexponential function that yielded time constants of 5800 s (70%) and 1100 s (30%) (Figure 2, inset). The fit is in excellent agreement with the data

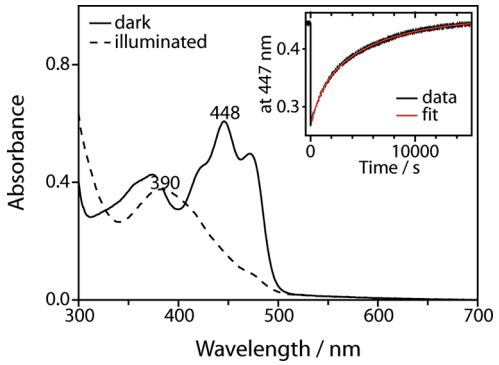

Figure 2. UV−vis spectrum of LOV-JαΔA′α in the dark (—) and after illumination for 10 s (---). The absorbance spectrum in the dark shows the typical fine structure of protein-bound oxidized flavin with an absorption maximum at 448 nm. Illumination leads to the formation of the adduct state, which is indicated by the absorption maximum at 390 nm. The inset shows the recovery kinetics of LOV-JαΔA′α at 447 nm after illumination for 500 ms (black line). Time constants of 5800 s (70%) and 1100 s (30%) were determined by fitting with a biexponential function (red line).

(R^2 = 0.99988). The slower and faster time constants showed a maximal deviation over several experiments of 8% and 20%, respectively. In a previous study, the recovery kinetics of A′α-LOV-Jα of aureochrome1a, containing both the A′α helix and the Jα helix, was recorded under the same conditions and exhibited time constants of 2290 s (86%) and 320 s (14%).[17] Therefore, deletion of the A′α helix led to an ∼3-fold slower recovery kinetics.

The influence of the A′α helix on the oligomerization of the LOV domain in the dark and under illumination was analyzed via size exclusion chromatography (SEC) on LOV-JαΔA′α at concentrations of 0.2, 0.5, and 2.5 mM (Figure 3). Absorbance was simultaneously detected at 448 and 390 nm, where only protein with chromophore absorbs. At these two wavelengths, absorbance coefficients differ for the dark and light states and therefore result in differences in absorbance in the elution profile. In the oxidized dark state, flavin absorbs by a factor of 2 less at 390 nm than at 448 nm, whereas in the light state, the flavin−cysteine adduct absorbs mainly at 390 nm and 5 times less at 448 nm. The SEC at a concentration of 0.2 mM showed a maximum at an elution volume of 12.1 mL in the dark (Figure 3A), which corresponds to an apparent molecular mass of 26 kDa. Considering a theoretical molecular mass of 16.8 kDa, the maximum can be assigned to a monomer of flavin-containing LOV-JαΔA′α. Additionally, a shoulder at 11.5 mL is present, which points to a dimeric species with an apparent mass of 36 kDa. Some aggregates were observed at the exclusion volume of the column at 8.6 mL. The formation of higher-order oligomers was excluded, because this fraction eluted even with a Superdex200 column at the exclusion volume of >600 kDa (Figure S3 of the Supporting Information). The simultaneous observation of a monomeric and a dimeric species points to a concentration-dependent equilibrium in the dark.

An increase in the starting concentration of SEC to 0.5 mM led to elution of a single peak with a strong shift of the maximum to 11.7 mL (33 kDa), which is intermediary between those of the monomer and dimer (Figure 3B). Such a shift points to a scenario in which the association and dissociation rates of the dimer are faster than the chromatography run time, which leads to a concentration-dependent shift of the elution peaks of monomer and dimer toward intermediate elution

DOI: 10.1021/bi501509z
Biochemistry 2015, 54, 1484−1492

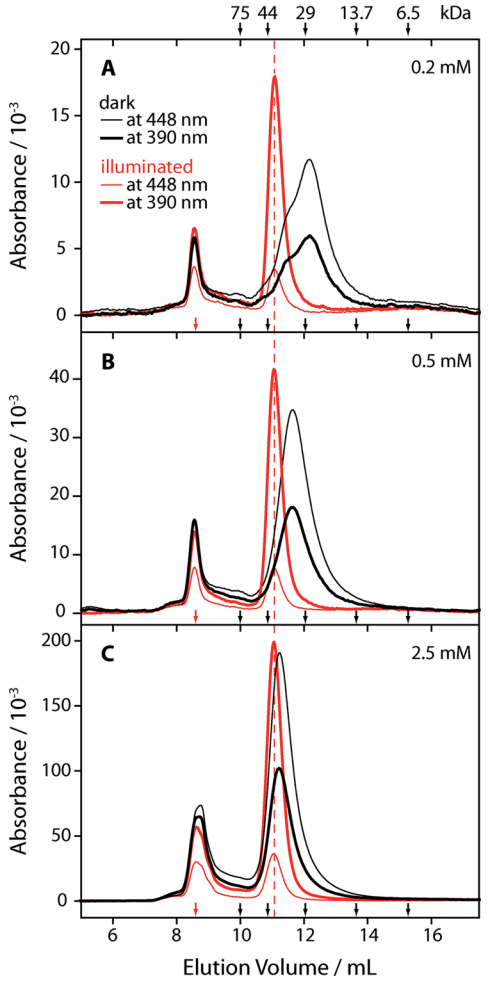

Figure 3. Size exclusion chromatography of LOV-J$\alpha$$\Delta$A′$\alpha$ at injected concentrations of 0.2, 0.5, and 2.5 mM in the dark (black lines) and under continuous illumination (red lines). Protein with bound chromophore was detected at 448 nm (thin line) and 390 nm (thick line). (A) At a concentration of 0.2 mM in the dark, LOV-J$\alpha$$\Delta$A′$\alpha$ eluted with a maximum at 12.1 mL and a shoulder at 11.5 mL, which corresponds to apparent molecular masses of 26 and 36 kDa, respectively. With a theoretical molecular mass of 16.8 kDa, the former can be assigned to a monomeric species and latter to a dimeric species. (B) At 0.5 mM in the dark, the elution maximum shifted to 11.7 mL (33 kDa), which is intermediary between those of the monomer and dimer. (C) At 2.5 mM in the dark, LOV-J$\alpha$$\Delta$A′$\alpha$ eluted at 11.2 mL (41 kDa), which is consistent with the molecular mass of a dimer. In conclusion, LOV-J$\alpha$$\Delta$A′$\alpha$ shows a concentration-dependent equilibrium between the monomer and dimer in the dark. Under continuous illumination, LOV-J$\alpha$$\Delta$A′$\alpha$ eluted as a dimer at 11.2 mL (44 kDa) at all three concentrations. The void volume was 8.6 mL as determined by the elution volume of ferritin (440 kDa) and is marked by an arrow (red). The elution volumes of protein standards used for calibration are further marked by arrows (black). From left to right: conalbumin (75 kDa), ovalbumin (44 kDa), carbonic anhydrase (29 kDa), ribonuclease A (13.7 kDa), and aprotinin (6.5 kDa), respectively.

volumes.[27] When the concentration was further increased 5-fold to 2.5 mM, LOV-J$\alpha$$\Delta$A′$\alpha$ eluted as a single, narrow peak with a maximum at 11.2 mL (41 kDa), which is consistent with the molecular mass of the dimer (Figure 3C). Consequently, LOV-J$\alpha$$\Delta$A′$\alpha$ forms dimers in the dark at all investigated concentrations. As the chromophore occupancy was ~20%, the detected dimeric species are mostly composed of holoprotein and apoprotein. The possibility that the affinity for the association of a fully occupied dimer in the dark might differ cannot be excluded. Nevertheless, the deletion of the A′α helix allowed a dimerization of the LOV domains in the dark, because A′α-LOV-Jα at the same chromophore occupancy was present in the dark as a monomer even at high concentrations.[17] We conclude that the A′α helix covers the dimerization site of the LOV domain, which then becomes permanently exposed by truncation in LOV-J$\alpha$$\Delta$A′$\alpha$.

Under continuous illumination, LOV-J$\alpha$$\Delta$A′$\alpha$ eluted at 11.1 mL at all three concentrations (Figure 3). This volume corresponds to an apparent mass of 44 kDa and can therefore be assigned to a dimer. At the lowest concentration of 0.2 mM, flavin-containing LOV-J$\alpha$$\Delta$A′$\alpha$ is mainly monomeric in the dark but dimeric in the light state. Therefore, the binding affinity for dimerization increases upon illumination, which is significant for the dark reversion of the receptor (see Discussion). The light-induced dimer shows an apparent mass that is 3 kDa higher than that of the dark-state dimer at high concentrations. The shift of the elution peak might be explained by the rapid dissociation of the dimer relative to the chromatography run time. However, the contribution by monomers to the profile is considered to be small relative to this significant shift of 0.9 mL. A more likely explanation is that most of this upshift is caused by a secondary structural change in the light state in the LOV core. This interpretation is supported by the previous, similar finding that A′α-LOV showed a reproducible and concentration-independent increase in the apparent mass of the monomer of 2 kDa upon illumination.[17]

To investigate the influence of the A′α helix on the light-induced changes in secondary structure of A′α-LOV-Jα, LOV-J$\alpha$$\Delta$A′$\alpha$ was subjected to FT-IR difference spectroscopy. The results were analyzed by comparison to those previously obtained on A′α-LOV-Jα and A′α-LOV.[17] This systematic approach allows for a segment-resolved assignment of bands in the double difference spectrum, as it has been demonstrated for phototropin.[28] All spectra were recorded under the same conditions and were scaled to the bands at 1303, 1272, and 1251 cm^{-1} (Figure 4A). In this region, bands originate from the flavin chromophore and are typical for LOV domains.[29−31] Only those bands are visible in the difference spectra that originate from light-induced structural changes in the chromophore or the protein moiety. Negative bands originate from the dark state and positive bands from the light state. Significant deviations among the three difference spectra are mainly found in the amide I region between 1615 and 1695 cm^{-1} and in the amide II region between 1520 and 1570 cm^{-1}. Exclusively in these regions, light-induced secondary structural changes can be detected by infrared spectroscopy.[32]

A pronounced negative band at 1643 cm^{-1} is found in the difference spectra of both LOV-J$\alpha$$\Delta$A′$\alpha$ and A′α-LOV-Jα (Figure 4A). In contrast, a band with much less intensity is detected at the same position in the difference spectrum of A′α-LOV, which has previously been assigned to a moderate amide I signal of the LOV core in phototropin2-LOV2 from *A. thaliana* and neochrome1-LOV2 from *Adiantum capillus-veneris*.[29,33] The additional negative signal at 1643 cm^{-1} in the difference spectrum of LOV-J$\alpha$$\Delta$A′$\alpha$ and A′α-LOV-Jα is detected far above the noise level and the extent of sample-to-sample variation. In a previous study, this signal has accordingly been assigned to an unfolding of the Jα helix,[17] in agreement with studies of other LOV domains with similar band positions of this helix.[28,33−35] It should be noted that an alternative

DOI: 10.1021/bi501509z
Biochemistry 2015, 54, 1484−1492

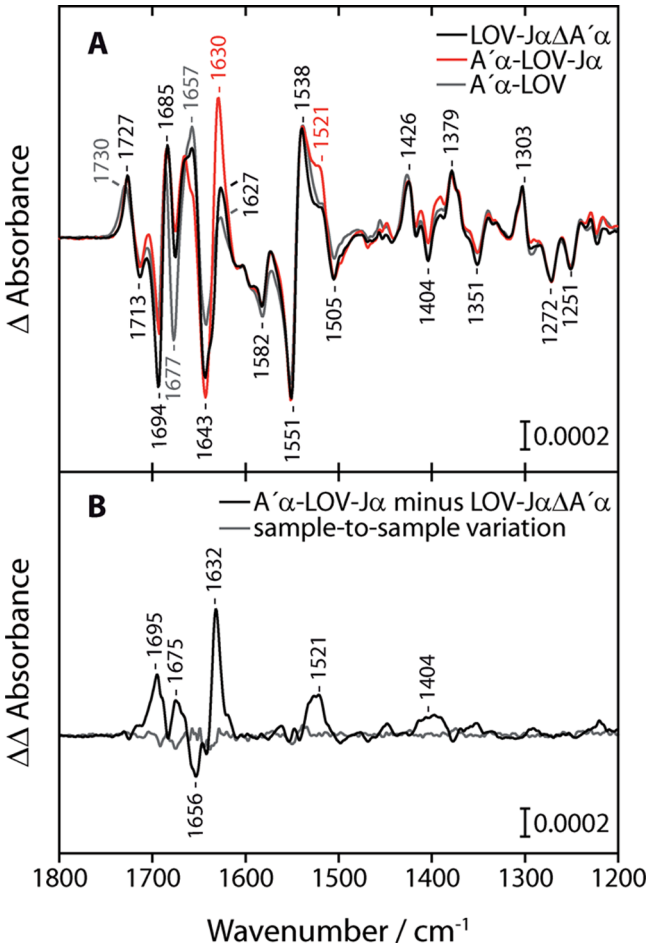

Figure 4. (A) Light-minus-dark FT-IR difference spectrum of LOV-JαΔA′α (black) in comparison to those of A′α-LOV-Jα (red) and A′α-LOV (gray) taken from ref 17. Light-induced unfolding of the Jα helix takes place in LOV-JαΔA′α as is evidenced by the negative band at 1643 cm^{-1}. (B) Segment-resolved double difference spectrum obtained by subtraction of the difference spectrum of LOV-JαΔA′α from that of A′α-LOV-Jα (black). The contribution of the A′α helix of A′α-LOV-Jα is evident at 1656 cm^{-1}. Its negative sign points to an unfolding upon illumination. The prominent positive band at 1632 cm^{-1} represents a marker band for light-induced dimerization in A′α-LOV-Jα. The double difference spectrum of LOV-JαΔA′α minus LOV-JαΔA′α illustrates the sample-to-sample variation of independent preparations.

increase in the intensity of the signal from the LOV core has to be based on additional amide elements of a helix responding to the light. Such an extension of a helix, however, would be accompanied by a downshift in frequency of the coupled amide I signal.[36,37] Consequently, the Jα helix unfolds upon illumination even in the absence of the A′α helix. The intensity of the corresponding band is reduced in the difference spectrum of LOV-JαΔA′α compared to that of A′α-LOV-Jα, which might be rationalized by a partial unfolding of the Jα helix in the dark in the absence of A′α. A similar reduction in the extent of undocking of the Jα helix was observed by CD spectroscopy in the corresponding LOV-JαΔA′α of phototropin1 from *Av. sativa*.[22]

To isolate specific signals that originate from the deletion of the A′α helix, a double difference spectrum was calculated by subtracting the difference spectrum of LOV-JαΔA′α from that of A′α-LOV-Jα (Figure 4B). Thereby, signals from the flavin chromophore cancel each other out. The remaining bands in the double difference spectrum originate from either structural changes in the A′α helix itself or structural changes that depend on the presence of the A′α helix. There is only one band found in the region of the double difference spectrum in which α-helices absorb.[32] This band is located at 1656 (−) cm^{-1} and can therefore be assigned to the A′α helix (Table 1). The negative

Table 1. Assignment of FT-IR Difference Bands of *Pt*AUREO1a-A′α-LOV-Jα in the Amide I and Amide II Spectral Region (1695−1520 cm^{-1})[a]

dark state (negative band)	light state (positive band)	assignment
	1695	amide I, β-sheet
1694		C_4=O stretch of FMN[b]
	1685	C_2=O stretch of FMN[c]
1677		C_2=O stretch of FMN[c]
	1677	amide I, increase in turn structure, propagation from Jα to A′α helix
1656		amide I, A′α unfolding
1643		amide I, Jα unfolding
	1630	amide I, dimerization at the β-sheet surface
1582		C_{4a}=N_5,[c,d] C=C,[d] C_{10a}=N_1[d] stretches of FMN
1551		C_{10a}=N_1,[c,d] C_{10a}=N_{10},[d] C=C[d] stretches of FMN and amide II
	1538	C_{10a}=N_1[c] stretch of FMN and amide II
	1521	C_{10a}=N_1[c] stretch of FMN and amide II

[a]Band positions are given in inverse centimeters. [b]From ref 34. [c]From ref 29. [d]From ref 44.

sign points to an unfolding of the A′α helix in A′α-LOV-Jα upon illumination. To the best of our knowledge, the IR signal of A′α unfolding is identified here for the first time. The position of the signal is upshifted in frequency as compared to that of the Jα helix at 1643 cm^{-1}, which is in agreement with the general observation that shorter helices absorb at higher frequencies within the spectral range specific for α-helices.[36,37] It has previously been suggested that an unfolding of the A′α helix in A′α-LOV-Jα might take place, because this band at 1656 cm^{-1} was observed in the double difference spectrum of A′α-LOV-Jα minus A′α-LOV.[17] The latter observations imply that the A′α helix unfolds only in A′α-LOV-Jα but not in LOV-JαΔA′α or A′α-LOV. Consequently, the A′α helix in A′α-LOV either does not unfold upon illumination or is already unfolded in the dark. The latter case can be excluded by the fact that A′α-LOV is a monomer in the dark,[17] which requires a folded A′α helix to cover the dimerization site. The presence of the Jα helix is therefore necessary to trigger the light-induced unfolding of the A′α helix. In contrast, the Jα helix unfolds even in the absence of the A′α helix, as can be seen in the difference spectrum of LOV-JαΔA′α at 1643 cm^{-1}. This unidirectional dependence implies a chronological sequence in the photoreaction of A′α-LOV-Jα, in which the Jα helix unfolds first and then triggers the unfolding of the A′α helix. In other words, the Jα helix acts as an allosteric activator for unfolding of the A′α helix.

The most pronounced band of all three difference spectra is a positive band at 1630 cm^{-1} found only for A′α-LOV-Jα (Figure 4A). Therefore, both flanking helices have to be present to induce this difference band, which is located in a spectral region specific for β-sheets.[32] The presence of the signal can be

DOI: 10.1021/bi501509z
Biochemistry 2015, 54, 1484−1492

directly correlated with the observation of light-induced dimerization, which requires that both helices be unfolded by light. Such a light-induced change at the dimer interface is expected only for A′α-LOV-Jα, because A′α-LOV does not dimerize[17] and LOV-JαΔA′α is already a dimer in the dark at the concentrations used in the IR experiments (Figure 3C). Dimerization most likely occurs at the β-sheet surface of the LOV core,[38−41] because the alternative contact surface provided by flanking helices[42,43] is lost by the observed unfolding. Therefore, the prominent positive band at 1630 (+) cm^{-1} in the difference spectrum of A′α-LOV-Jα (and at 1632 cm^{-1} in the double difference spectrum) represents a marker band for light-induced dimerization at the β-sheet surface (Table 1). It might be rationalized by an increase in oscillator strength by the intermolecular extension of the β-sheet network. The signal is accompanied by the typical weaker mode of β-sheets at higher frequencies[32] that contributes to the band at 1695 cm^{-1} (Figure 4B).

Besides the bands at 1695, 1656, and 1632 cm^{-1}, further bands in the spectrum of A′α-LOV-Jα depend on the presence of the A′α helix at 1675, 1521, and 1404 cm^{-1} (Figure 4B). To aid in their assignment, H/D exchange was performed for A′α-LOV-Jα (Figure 5). The efficient exchange is reflected by the

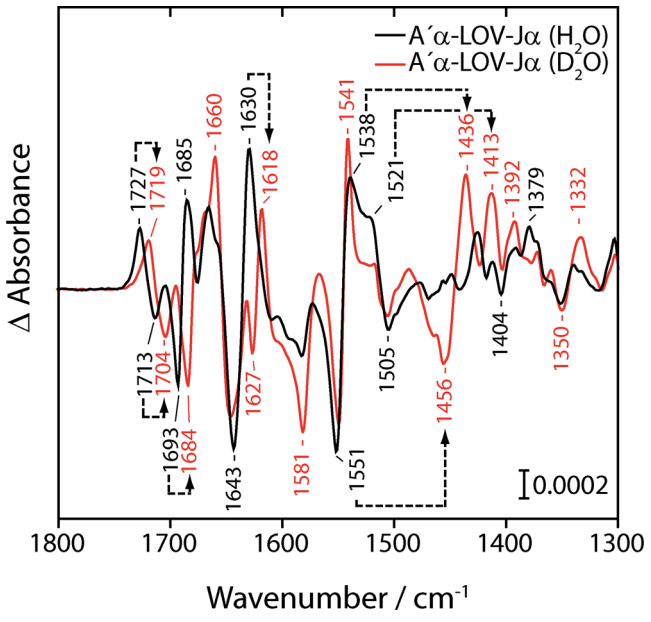

Figure 5. Light-minus-dark FT-IR difference spectra of A′α-LOV-Jα in D_2O (red) and H_2O (black). The efficient exchange of hydrogen and deuterium is demonstrated by the shift of C_4O bands of flavin from 1727, 1713, and 1693 cm^{-1} to 1719, 1704, and 1684 cm^{-1}, respectively. Bands at 1456, 1436, and 1413 cm^{-1} in D_2O are assigned to amide II′ bands of corresponding amide II bands in H_2O that contribute to the bands at 1551, 1538, and 1521 cm^{-1}, respectively. Amide II bands originate from changes in secondary structure.

large shift of 9 cm^{-1} of the C_4O bands of flavin to 1704 (−) and 1684 (−) cm^{-1}. The extent of the downshift is in full agreement with quantum chemical calculations on oxidized lumiflavin.[44] The spectral range of 1680−1640 cm^{-1} cannot be finally evaluated here because of the strong overlap of amide I bands and flavin bands. The β-sheet signal at 1630 cm^{-1} shifts to 1618 cm^{-1}. The band at 1521 (+) cm^{-1} exhibits a pronounced shift most likely to 1413 (+) cm^{-1}. Therefore, this band is assigned to an amide II vibration (Table 1), for which a downshift of ∼100 cm^{-1} is characteristic.[32] Similarly, bands at 1551 (−) and 1538 (+) cm^{-1} in the difference spectrum of A′α-LOV-Jα in H_2O contain contributions of amide II vibrations (Table 1), which strongly absorb in D_2O at 1456 (−) and 1436 (+) cm^{-1}. The origin of the band at 1404 (+) cm^{-1} in the double difference spectrum remains to be assigned. In summary, the pronounced changes in conformation of A′α-LOV-Jα upon illumination are reflected in the strong contributions identified in the amide II range of the difference spectrum.

DISCUSSION

The role of the A′α helix in aureochrome requires special attention because the helix participates in the covalent connection between the sensory LOV domain and its effector domain. In contrast, the role of the A′α helix in signaling of phototropin has long been overlooked because of its location distant from the effector in the primary sequence. Only recently, a partial destabilization of the Jα helix upon truncation of the A′α helix but not vice versa was found in phototropin1-LOV2 from *Av. sativa* and *A. thaliana*,[22,23] which is in full agreement with the observations on aureochrome-LOV made in this study. Furthermore, all three LOV domains similarly exhibit a light-induced unfolding of both the A′α helix and the Jα helix. However, the flanking helices of phototropin-LOV2 were shown to unfold independently of each other,[22,23] whereas unfolding of A′α in aureochrome-LOV takes place only in the presence and after unfolding of the Jα helix. The A′α helix remains folded in the dark and light upon truncation of the Jα helix. This finding implies a direct dependence of the unfolding of the A′α helix on that of the C-terminal Jα helix.

Allosteric Control of Unfolding of the A′α Helix by the Jα Helix in Aureochrome. The interdependence of A′α and Jα helices is most likely not realized by a direct contact. If unfolding of Jα would directly destabilize A′α, this would result in an unfolded A′α helix in A′α-LOV already in the dark. This possibility can be excluded by the fact that A′α-LOV is a monomer in the dark,[17] which requires a folded A′α helix covering the dimerization site. In support of this reasoning, these two helices do not directly interact with each other in the crystal structure of *V. frigida* aureochrome1-LOV.[15] These observations raise the question of how the signal propagates from the Jα helix to the A′α helix. Such an allosteric process in the LOV core might be based on general changes in flexibility or on a localized change in secondary structure. In the latter case, difference bands originating from the propagation of the signal from the Jα helix to the A′α helix would be present in the FT-IR spectra of A′α-LOV-Jα and LOV-JαΔA′α but would be missing in that of A′α-LOV. Such a strong difference in absorbance can be found at 1677 cm^{-1} (Figure 4A). The negative band in the spectrum of A′α-LOV results from the C_2O vibration of FMN[29,31] and is compensated by a positive contribution from the protein moiety in the spectra of A′α-LOV-Jα and LOV-JαΔA′α. This spectral region is specific for turn structural elements.[32] Therefore, the difference in absorbance at 1677 cm^{-1} is assigned to a strengthening of turn structure, which is associated with the propagation of the allosteric signal from the Jα helix to the A′α helix.

Change in Dimer Affinity by Light and Its Role in the Resetting of the Receptor. It was observed by SEC that illumination of LOV-JαΔA′α leads to an increase in the affinity of dimerization at the site covered by the A′α helix. The underlying conformational change linking this site with adduct

DOI: 10.1021/bi501509z
Biochemistry 2015, 54, 1484−1492

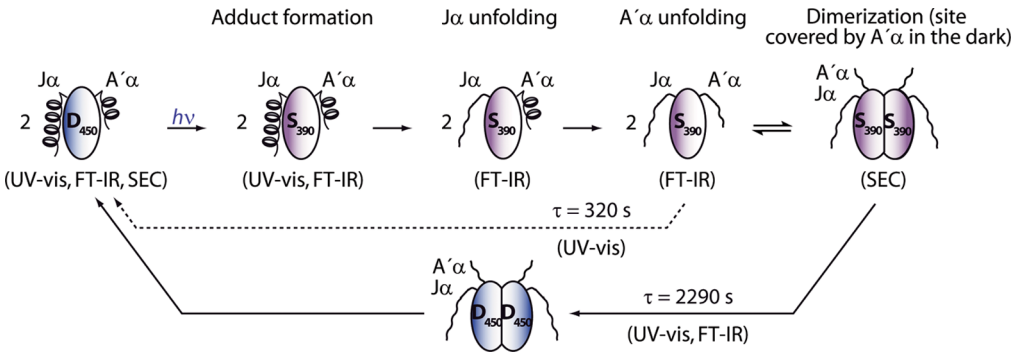

Figure 6. Model of the stepwise photoreaction of aureochrome-LOV. The LOV domain in its dark form (D_{450}) is monomeric with folded N- and C-terminal flanking helices A′α and Jα. After illumination, adduct state S_{390} is formed. As a first consequence, the signal propagates to the C-terminal Jα helix and triggers its unfolding. This process in the Jα helix allosterically induces the unfolding of the A′α helix. As the A′α helix covers the dimerization site, light-induced unfolding of the latter allows for a dimerization of two LOV domains in their light state. The adduct state thermally converts back into the oxidized state, in *Pt*AUREO1a with a major time constant of 2290 s. The photocycle is completed by dissociation of the dimer and refolding of the helices.

formation might be identical to that of the allosteric control of A′α unfolding by Jα (signal at 1677 cm^{-1}). The presence of an additional conformational change in the LOV core increasing the affinity cannot be excluded. After illumination, the affinity of the dimer decreases again concomitantly with the dark reversion of the chromophore. This process is of relevance for signaling because it clearly accelerates the necessary dissociation of the dimers in the dark and the recovery of the monomeric dark form of aureochrome-LOV.

Model of the Photoreaction of Aureochrome-LOV. Together with previous results,[17] this study allows us to draw the following picture of the processes taking place in aureochrome-LOV and its flanking helices A′α and Jα (Figure 6). In the dark, the LOV domain is monomeric and both helices are folded. The flavin chromophore is present in its oxidized state and then forms the adduct state upon illumination. Together with propagation of the signal to Jα, an increase in the overall shape takes place as observed by SEC (increase by 2 kDa). Consequent unfolding of the Jα helix then initiates an allosteric control of A′α helix unfolding through the LOV core, which is mediated by a change in turn structural elements. This process might additionally lead to the observed increase in affinity for dimerization. As the folded A′α helix covers the dimerization site in the dark, unfolding of the latter induces dimerization of two LOV domains in their light state. In the dark, the adduct state converts back into the oxidized state, for *Pt*AUREO1a with a major time constant of 2290 s. The photocycle is completed by dissociation of the dimer and refolding of the helices, which is facilitated by the decrease in the affinity for dimerization in the dark. The time constants of the latter processes need to be determined.

We expect that this scheme is also valid for other aureochrome-LOV domains with their flanking helices. Light-induced dimerization has additionally been demonstrated *in vivo* for aureochrome1-LOV from *V. frigida*, *Nannochloropsis gaditana*, and *Ochromonas danica* in an optogenetic approach in cells[16] as well as *in vitro* for *V. frigida* aureochrome1-LOV.[45] In the dark, *V. frigida* aureochrome1-LOV was observed to be a dimer at higher concentrations.[15,45,46] In contrast, A′α-LOV-Jα of *Pt*AUREO1a was observed as a monomer via SEC even at a starting concentration of 3.7 mM, albeit within the limited precision of this method.[17] Therefore, the dark activity of *Pt*AUREO1a-LOV might be comparably low, which makes it a promising candidate for such optogenetic approaches that benefit from light-induced dimerization.

Light-induced dimerization has also been observed for other LOV domains such as the bacterial LOV-HTH protein EL222 and the fungal receptor Vivid as well as phototropin2-LOV1 from *A. thaliana*.[42,47,48] In the latter two cases, the dark-state dimer was observed via SEC at comparably low concentrations (150 and 600 μM, respectively). The opposite effect, light-induced monomerization, was found for a short LOV protein from *Rhodobacter sphaeroides*.[49] Accordingly, the control of the LOV domain oligomeric state by light absorption might be a mechanism for regulating functions in LOV proteins more common than currently known.

Outlook for the Mechanism of Full-Length Aureochrome in Comparison to That of Phototropin. *In vivo* studies of phototropin showed that its LOV2-A′α helix plays an essential role for functionality.[20,21] In aureochromes, the congruence between the N-terminal position of the effector domain and the unfolding of the linking A′α helix in the photoreaction of the isolated LOV domain argues for a central role of the A′α helix in propagation of the signal to the bZIP domain. However, the allosteric control of the A′α helix by the Jα helix as well as the light-induced dimerization of the isolated LOV domain has not been found for phototropin-LOV2 and points to a different mechanism within the full-length proteins. In the two current models for light-induced DNA binding in *V. frigida* aureochrome1, dimerization of the LOV domains plays a central role. First, under reducing conditions, light-induced dimerization of the aureochrome monomer driven by the LOV domains enhances the affinity for DNA binding.[11] Second, under oxidizing conditions, aureochrome is present as a dimer in the dark facilitated by disulfide linkages at the bZIP domain and the linking region[11] and then responds like a seesaw under illumination by the interaction at the LOV domains.[45] It should be noted that *Pt*AUREO1a does not possess cysteine residues outside of the LOV domain, so that such a dependence of the mechanism on the redox status of the cell is not expected.

FT-IR spectroscopic experiments on full-length aureochromes in the absence and presence of DNA are necessary to substantiate and validate the current models. Valuable information about changes in amino side chains by light in the presence of DNA has already been obtained.[12] The determination of marker bands for light-induced dimerization of LOV as well as for Jα and A′α helix unfolding in this study

DOI: 10.1021/bi501509z
Biochemistry 2015, 54, 1484−1492

will strongly facilitate elucidation of the contribution of these processes to signaling in full-length aureochrome.

■ ASSOCIATED CONTENT

Supporting Information

SDS−PAGE of LOV-JαΔA′α, FT-IR difference spectra of reconstituted and nonreconstituted LOV-JαΔA′α, and size exclusion chromatography of LOV-JαΔA′α on a Superdex200 column. This material is available free of charge via the Internet at http://pubs.acs.org.

■ AUTHOR INFORMATION

Corresponding Author

*Phone: +49-521-106-2062. Fax: +49-521-106-2981. E-mail: tilman.kottke@uni-bielefeld.de.

Funding

Financial support by the Deutsche Forschungsgemeinschaft, FOR1261, Grant KO 3580/1-2, is acknowledged.

Notes

The authors declare no competing financial interest.

■ ACKNOWLEDGMENTS

We thank Ina Ehring for excellent technical assistance. T.K. acknowledges generous support by Thomas Hellweg. We thank Peter G. Kroth for providing us with the template plasmid.

■ ABBREVIATIONS

bZIP, basic-region leucine zipper; CD, circular dichroism; FMN, flavin mononucleotide; FT-IR, Fourier transform infrared; HTH, helix−turn−helix; LOV, light-, oxygen-, or voltage-sensitive; fwhm, full width at half-maximum; *Pt*AUREO1a, aureochrome1a from *P. tricornutum*; SEC, size exclusion chromatography.

■ REFERENCES

(1) Takahashi, F., Yamagata, D., Ishikawa, M., Fukamatsu, Y., Ogura, Y., Kasahara, M., Kiyosue, T., Kikuyama, M., Wada, M., and Kataoka, H. (2007) AUREOCHROME, a photoreceptor required for photomorphogenesis in stramenopiles. *Proc. Natl. Acad. Sci. U.S.A. 104*, 19625−19630.

(2) Ishikawa, M., Takahashi, F., Nozaki, H., Nagasato, C., Motomura, T., and Kataoka, H. (2009) Distribution and phylogeny of the blue light receptors aureochromes in eukaryotes. *Planta 230*, 543−552.

(3) Schellenberger Costa, B., Sachse, M., Jungandreas, A., Bartulos, C. R., Gruber, A., Jakob, T., Kroth, P. G., and Wilhelm, C. (2013) Aureochrome 1a Is Involved in the Photoacclimation of the Diatom *Phaeodactylum tricornutum*. *PLoS One 8*, e74451.

(4) Deng, Y., Yao, J., Fu, G., Guo, H., and Duan, D. (2014) Isolation, expression, and characterization of blue light receptor AUREOCHROME gene from *Saccharina japonica* (Laminariales, Phaeophyceae). *Mar. Biotechnol. 16*, 135−143.

(5) Huysman, M. J., Fortunato, A. E., Matthijs, M., Schellenberger Costa, B., Vanderhaeghen, R., Van den Daele, H., Sachse, M., Inze, D., Bowler, C., Kroth, P. G., Wilhelm, C., Falciatore, A., Vyverman, W., and De Veylder, L. (2013) AUREOCHROME1a-Mediated Induction of the Diatom-Specific Cyclin dsCYC2 Controls the Onset of Cell Division in Diatoms (*Phaeodactylum tricornutum*). *Plant Cell 25*, 215−228.

(6) Christie, J. M. (2007) Phototropin blue-light receptors. *Annu. Rev. Plant Biol. 58*, 21−45.

(7) Losi, A., and Gärtner, W. (2008) Shedding (blue) light on algal gene expression. *Proc. Natl. Acad. Sci. U.S.A. 105*, 7−8.

(8) Salomon, M., Christie, J. M., Knieb, E., Lempert, U., and Briggs, W. R. (2000) Photochemical and mutational analysis of the FMN-binding domains of the plant blue light receptor phototropin. *Biochemistry 39*, 9401−9410.

(9) Nijhawan, A., Jain, M., Tyagi, A. K., and Khurana, J. P. (2008) Genomic survey and gene expression analysis of the basic leucine zipper transcription factor family in rice. *Plant Physiol. 146*, 333−350.

(10) Ye, W., Wang, Y., Dong, S., Tyler, B. M., and Wang, Y. (2013) Phylogenetic and transcriptional analysis of an expanded bZIP transcription factor family in *Phytophthora sojae*. *BMC Genomics 14*, 839.

(11) Hisatomi, O., Nakatani, Y., Takeuchi, K., Takahashi, F., and Kataoka, H. (2014) Blue Light-induced Dimerization of Monomeric Aureochrome-1 Enhances Its Affinity for the Target Sequence. *J. Biol. Chem. 289*, 17379−17391.

(12) Kerruth, S., Ataka, K., Frey, D., Schlichting, I., and Heberle, J. (2014) Aureochrome 1 illuminated: Structural changes of a transcription factor probed by molecular spectroscopy. *PLoS One 9*, e103307.

(13) Crosson, S., Rajagopal, S., and Moffat, K. (2003) The LOV domain family: Photoresponsive signaling modules coupled to diverse output domains. *Biochemistry 42*, 2−10.

(14) Losi, A., and Gärtner, W. (2008) Bacterial bilin- and flavin-binding photoreceptors. *Photochem. Photobiol. Sci. 7*, 1168−1178.

(15) Mitra, D., Yang, X., and Moffat, K. (2012) Crystal Structures of Aureochrome1 LOV Suggest New Design Strategies for Optogenetics. *Structure 20*, 698−706.

(16) Grusch, M., Schelch, K., Riedler, R., Reichhart, E., Differ, C., Berger, W., Inglés-Prieto, A., and Janovjak, H. (2014) Spatio-temporally precise activation of engineered receptor tyrosine kinases by light. *EMBO J. 33*, 1713−1726.

(17) Herman, E., Sachse, M., Kroth, P. G., and Kottke, T. (2013) Blue-Light-Induced Unfolding of the Jα Helix Allows for the Dimerization of Aureochrome-LOV from the Diatom *Phaeodactylum tricornutum*. *Biochemistry 52*, 3094−3101.

(18) Harper, S. M., Neil, L. C., and Gardner, K. H. (2003) Structural basis of a phototropin light switch. *Science 301*, 1541−1544.

(19) Harper, S. M., Christie, J. M., and Gardner, K. H. (2004) Disruption of the LOV-Jα helix interaction activates phototropin kinase activity. *Biochemistry 43*, 16184−16192.

(20) Aihara, Y., Yamamoto, T., Okajima, K., Yamamoto, K., Suzuki, T., Tokutomi, S., Tanaka, K., and Nagatani, A. (2012) Mutations in N-terminal flanking region of blue light-sensing light-oxygen and voltage 2 (LOV2) domain disrupt its repressive activity on kinase domain in the *Chlamydomonas* phototropin. *J. Biol. Chem. 287*, 9901−9909.

(21) Sharma, S., Kharshiing, E., Srinivas, A., Zikihara, K., Tokutomi, S., Nagatani, A., Fukayama, H., Bodanapu, R., Behera, R. K., Sreelakshmi, Y., and Sharma, R. (2014) A dominant mutation in the light-oxygen and voltage2 domain vicinity impairs phototropin1 signaling in tomato. *Plant Physiol. 164*, 2030−2044.

(22) Zayner, J. P., Antoniou, C., and Sosnick, T. R. (2012) The amino-terminal helix modulates light-activated conformational changes in *As*LOV2. *J. Mol. Biol. 419*, 61−74.

(23) Takeda, K., Nakasone, Y., Zikihara, K., Tokutomi, S., and Terazima, M. (2013) Dynamics of the amino-terminal and carboxyl-terminal helices of *Arabidopsis* phototropin 1 LOV2 studied by the transient grating. *J. Phys. Chem. B 117*, 15606−15613.

(24) Depauw, F. A., Rogato, A., Ribera d'Alcala, M., and Falciatore, A. (2012) Exploring the molecular basis of responses to light in marine diatoms. *J. Exp. Bot. 63*, 1575−1591.

(25) Nelson, D. M., Treguer, P., Brzezinski, M. A., Leynaert, A., and Queguiner, B. (1995) Production and Dissolution of Biogenic Silica in the Ocean: Revised Global Estimates, Comparison with Regional Data and Relationship to Biogenic Sedimentation. *Global Biogeochem. Cycles 9*, 359−372.

(26) Macheroux, P. (1999) UV-visible spectroscopy as a tool to study flavoproteins. *Methods Mol. Biol. 131*, 1−7.

(27) Stevens, F. J. (1989) Analysis of protein-protein interaction by simulation of small-zone size exclusion chromatography. Stochastic formulation of kinetic rate contributions to observed high-performance

DOI: 10.1021/bi501509z
Biochemistry 2015, 54, 1484−1492

liquid chromatography elution characteristics. *Biophys. J. 55*, 1155−1167.
(28) Pfeifer, A., Mathes, T., Lu, Y., Hegemann, P., and Kottke, T. (2010) Blue light induces global and localized conformational changes in the kinase domain of full-length phototropin. *Biochemistry 49*, 1024−1032.
(29) Iwata, T., Nozaki, D., Sato, Y., Sato, K., Nishina, Y., Shiga, K., Tokutomi, S., and Kandori, H. (2006) Identification of the C═O Stretching Vibrations of FMN and Peptide Backbone by ^{13}C-Labeling of the LOV2 Domain of *Adiantum* Phytochrome3. *Biochemistry 45*, 15384−15391.
(30) Swartz, T. E., Wenzel, P. J., Corchnoy, S. B., Briggs, W. R., and Bogomolni, R. A. (2002) Vibration spectroscopy reveals light-induced chromophore and protein structural changes in the LOV2 domain of the plant blue-light receptor phototropin 1. *Biochemistry 41*, 7183−7189.
(31) Ataka, K., Hegemann, P., and Heberle, J. (2003) Vibrational Spectroscopy of an Algal Phot-LOV1 Domain Probes the Molecular Changes Associated with Blue-Light Reception. *Biophys. J. 84*, 466−474.
(32) Barth, A., and Zscherp, C. (2002) What vibrations tell us about proteins. *Q. Rev. Biophys. 35*, 369−430.
(33) Koyama, T., Iwata, T., Yamamoto, A., Sato, Y., Matsuoka, D., Tokutomi, S., and Kandori, H. (2009) Different role of the Jα helix in the light-induced activation of the LOV2 domains in various phototropins. *Biochemistry 48*, 7621−7628.
(34) Alexandre, M. T., van Grondelle, R., Hellingwerf, K. J., and Kennis, J. T. (2009) Conformational heterogeneity and propagation of structural changes in the LOV2/Jα domain from *Avena sativa* phototropin 1 as recorded by temperature-dependent FTIR spectroscopy. *Biophys. J. 97*, 238−247.
(35) Yamamoto, A., Iwata, T., Sato, Y., Matsuoka, D., Tokutomi, S., and Kandori, H. (2009) Light signal transduction pathway from flavin chromophore to the Jα helix of *Arabidopsis* phototropin1. *Biophys. J. 96*, 2771−2778.
(36) Dousseau, F., and Pézolet, M. (1990) Determination of the Secondary Structure-Content of Proteins in Aqueous-Solutions from Their Amide-I and Amide-II Infrared Bands: Comparison Between Classical and Partial Least-Squares Methods. *Biochemistry 29*, 8771−8779.
(37) Torii, H., and Tasumi, M. (1992) Application of the 3-Dimensional Doorway-State Theory to Analyses of the Amide-I Infrared Bands of Globular-Proteins. *J. Chem. Phys. 97*, 92−98.
(38) Buttani, V., Losi, A., Eggert, T., Krauss, U., Jaeger, K. E., Cao, Z., and Gärtner, W. (2007) Conformational analysis of the blue-light sensing protein YtvA reveals a competitive interface for LOV-LOV dimerization and interdomain interactions. *Photochem. Photobiol. Sci. 6*, 41−49.
(39) Möglich, A., and Moffat, K. (2007) Structural basis for light-dependent signaling in the dimeric LOV domain of the photosensor YtvA. *J. Mol. Biol. 373*, 112−126.
(40) Nakasako, M., Zikihara, K., Matsuoka, D., Katsura, H., and Tokutomi, S. (2008) Structural basis of the LOV1 dimerization of *Arabidopsis* phototropins 1 and 2. *J. Mol. Biol. 381*, 718−733.
(41) Rinaldi, J., Gallo, M., Klinke, S., Paris, G., Bonomi, H. R., Bogomolni, R. A., Cicero, D. O., and Goldbaum, F. A. (2012) The β-scaffold of the LOV domain of the *Brucella* light-activated histidine kinase is a key element for signal transduction. *J. Mol. Biol. 420*, 112−127.
(42) Zoltowski, B. D., and Crane, B. R. (2008) Light activation of the LOV protein Vivid generates a rapidly exchanging dimer. *Biochemistry 47*, 7012−7019.
(43) Circolone, F., Granzin, J., Jentzsch, K., Drepper, T., Jaeger, K. E., Willbold, D., Krauss, U., and Batra-Safferling, R. (2012) Structural basis for the slow dark recovery of a full-length LOV protein from *Pseudomonas putida*. *J. Mol. Biol. 417*, 362−374.
(44) Spexard, M., Thöing, C., Beel, B., Mittag, M., and Kottke, T. (2014) Response of the Sensory Animal-like Cryptochrome aCRY to Blue and Red Light As Revealed by Infrared Difference Spectroscopy. *Biochemistry 53*, 1041−1050.
(45) Toyooka, T., Hisatomi, O., Takahashi, F., Kataoka, H., and Terazima, M. (2011) Photoreactions of aureochrome-1. *Biophys. J. 100*, 2801−2809.
(46) Hisatomi, O., Takeuchi, K., Zikihara, K., Ookubo, Y., Nakatani, Y., Takahashi, F., Tokutomi, S., and Kataoka, H. (2012) Blue Light-Induced Conformational Changes in a Light-Regulated Transcription Factor, Aureochrome-1. *Plant Cell Physiol. 54*, 93−106.
(47) Zoltowski, B. D., Motta-Mena, L. B., and Gardner, K. H. (2013) Blue light-induced dimerization of a bacterial LOV-HTH DNA-binding protein. *Biochemistry 52*, 6653−6661.
(48) Nakasone, Y., Kawaguchi, Y., Kong, S. G., Wada, M., and Terazima, M. (2014) Photoinduced Oligomerization of *Arabidopsis thaliana* Phototropin 2 LOV1. *J. Phys. Chem. B 118*, 14314−14325.
(49) Conrad, K. S., Bilwes, A. M., and Crane, B. R. (2013) Light-induced subunit dissociation by a light-oxygen-voltage domain photoreceptor from *Rhodobacter sphaeroides*. *Biochemistry 52*, 378−391.

DOI: 10.1021/bi501509z
Biochemistry 2015, 54, 1484−1492